Changes in BiP availability reveal hypersensitivity to acute endoplasmic reticulum stress in cells expressing mutant huntingtin

Patrick Lajoie and Erik L. Snapp

Journal of Cell Science 125, 789

doi:10.1242/jcs.107870

There was an error published in *J. Cell Sci.* **124**, 3332-3343.

The source of the parent plasmid, the BiP-169 luciferase template plasmid derived from the rat *Grp78* promoter subfragment, used to create our ERSE Td Tomato ODC reporter was incorrectly attributed. The parent plasmid was originally described previously (Luo and Lee, 2002). We are grateful to Dr Amy S. Lee, University of Southern California, for providing the plasmid.

The authors apologise for this error.

Reference

Luo, S. and Lee, A. S. (2002). Requirement of the p38 mitogen-activated protein kinase signalling pathway for the induction of the 78 kDa glucose-regulated protein/immunoglobulin heavy-chain binding protein by azetidine stress: activating transcription factor 6 as a target for stress-induced phosphorylation. *Biochem. J.* **366**, 787-795.

Changes in BiP availability reveal hypersensitivity to acute endoplasmic reticulum stress in cells expressing mutant huntingtin

Patrick Lajoie and Erik L. Snapp*

Department Anatomy and Structural Biology, Albert Einstein College of Medicine of Yeshiva University, Bronx, NY 10461, USA

*Author for correspondence (erik-lee.snapp@einstein.yu.edu)

Accepted 17 May 2011
Journal of Cell Science 124, 3332–3343

doi: 10.1242/jcs.087510

Summary

Huntington's disease (HD) is caused by expanded glutamine repeats within the huntingtin (Htt) protein. Mutant Htt (mHtt) in the cytoplasm has been linked to induction of the luminal endoplasmic reticulum (ER) stress pathway, the unfolded protein response (UPR). How mHtt impacts the susceptibility of the ER lumen to stress remains poorly understood. To investigate molecular differences in the ER in cells expressing mHtt, we used live-cell imaging of a sensitive reporter of the misfolded secretory protein burden, GFP fused to the ER chaperone BiP (also known as GRP78), which decreases in mobility as it binds increasing amounts of misfolded proteins. Striatal neurons expressing full-length mHtt showed no differences in BiP–GFP mobility and no evidence of UPR activation compared with wild-type cells at steady state. However, mHtt-expressing cells were acutely sensitive to misfolded secretory proteins. Treatment with ER stressors, tunicamycin or DTT, rapidly decreased BiP–GFP mobility in mHtt striatal cells and accelerated UPR activation compared with wild-type cells. mHtt-expressing cells exhibited decreased misfolded protein flux as a result of ER associated degradation (ERAD) dysfunction. Furthermore, UPR-adapted mHtt cells succumbed to misfolded protein stresses that could be tolerated by adapted wild-type cells. Thus, mHtt expression impairs misfolded secretory protein turnover, decreases the ER stress threshold, and increases cell vulnerability to insults.

Key words: BiP, ERAD, FRAP, Huntingtin, UPR

Introduction

The ability of a cell to detect and respond to various stresses is crucial for cell survival. To cope with misfolded protein accumulation, cells have developed complex quality control (QC) mechanisms that assist correct protein folding in the endoplasmic reticulum (ER). Folding factors termed chaperones bind unfolded secretory proteins and help prevent them from misfolding and aggregating in the ER. In some cases, chaperones and QC machinery target misfolded proteins for destruction by the ER associated degradation (ERAD) pathway (Meusser et al., 2005). Accumulation of misfolded secretory proteins can activate the unfolded protein response (UPR), which has three major outcomes. First, the UPR transiently attenuates global protein translation to decrease the nascent protein burden (Harding et al., 1999). Second, the UPR triggers ER membrane expansion leading to an increased ER volume (Bernales et al., 2006; Schuck et al., 2009). Third, the UPR helps re-establish homeostasis by improving the capacity of the ER for secretory protein flux by upregulating levels of ER chaperones [including BiP (also known as 78 kDa glucose-regulated protein, GRP78) and GRP94] (Kozutsumi et al., 1988), translocon components (Martinez and Chrispeels, 2003), secretory vesicle forming proteins (Higashio and Kohno, 2002), and ERAD components (Gregersen and Bross, 2010). Failure to resolve the misfolded protein burden can lead to cell death (Tabas and Ron, 2011). Chronic activation of the UPR has been linked to a number of major diseases and conditions including diabetes, heart diseases, neurodegenerative diseases and aging (Marciniak and Ron, 2006; Scheper and Hoozemans, 2009). Therefore, modulation of the UPR is an emerging focus for developing therapeutics (Hosoi and Ozawa, 2010; Ozcan et al., 2006).

Huntington's disease (HD) is an autosomal dominant neurodegenerative disease that results from the expansion of a stretch of polyglutamines (polyQ) within the huntingtin protein (Htt) (Sturrock and Leavitt, 2010). Humans with more than 36 glutamine repeats will eventually show HD symptoms (Gusella and MacDonald, 2006). A prominent feature of HD and other polyQ disorders is the propensity of the mutant proteins to assemble into cytoplasmic insoluble amyloid-like fibrils termed inclusion bodies (IBs) (Chen et al., 2001; Scherzinger et al., 1999).

Many cellular pathways are impaired in cells expressing aberrant polyQ expanded proteins including: gene transcription (Riley and Orr, 2006), vesicular trafficking (Caviston and Holzbaur, 2009), mitochondrial function (Oliveira, 2010) and protein degradation (Finkbeiner and Mitra, 2008). In addition, ER stress has been implicated as an important contributor to polyQ toxicity in cells (Kouroku et al., 2002; Nishitoh et al., 2002; Thomas et al., 2005). Several methods have been used to detect ER stress induction in HD cells. Striatal cells, derived from the knockin mouse expressing 111 polyQ repeats, showed increased conavalin-A-reactive ER membranes, a feature associated with

ER stress (Trettel et al., 2000). Expression of Htt N-terminal fragments upregulated UPR markers and increased cell death (Reijonen et al., 2008). Upregulation of Rrs1 by ER stress in neurons of animal expressing mutant Htt (mHtt) also suggested a link between ER stress and HD (Carnemolla et al., 2009). Inhibition of apoptosis signal-regulating kinase 1 decreased ER stress in the R6/2 mouse, which expresses exon 1 of the human HD gene, containing 150 CAG repeats (Cho et al., 2009). Expression of mHtt increased levels of SCAM5 in neuronal cells through induction of ER stress pathways (Noh et al., 2009). Finally, data from both yeast and mammalian cell models of HD have shown ER stress and impaired ERAD associated with polyQ toxicity (Duennwald and Lindquist, 2008).

Most studies of ER stress in HD have focused on the downstream consequences of ER stress, such as upregulation of UPR markers including BiP and CHOP and the impact of UPR activation on cell survival (Carnemolla et al., 2009; Cho et al., 2009; Duennwald and Lindquist, 2008; Reijonen et al., 2008). However, how cytoplasmic mHtt impacts the function and molecular organization of the ER environment of neuronal cells remains poorly understood. Although several studies have reported associations between mHtt and ER stress, differences in models and choices of reporters of ER stress have raised questions of the relevance of the findings to HD. It is unclear whether mHtt causes ER stress or regulates the UPR sensors or effectors. The UPR is a response to the stress of misfolded secretory protein accumulation. However, the three UPR sensors, ATF6, Ire1 and PERK, are all resident ER membrane proteins with cytoplasmically exposed effector domains (Ron and Walter, 2007). Cytoplasmic mHtt could somehow regulate these sensors independently of luminal misfolded protein levels. In addition, cell death, a frequently used measure of UPR consequences and mHtt toxicity, is a late UPR event mediated by several cytoplasmic proteins and could also be regulated by cytoplasmic mHtt.

In this study we sought to characterize the impact of Htt expression on the ability of the ER to maintain homeostasis and respond to acute misfolded protein stress. By imaging fluorescent reporters in single cells we asked: (1) is the occupancy and availability of the ER QC machinery, especially ER chaperones, affected by mHtt expression? (2) does the ER environment in cells expressing wild-type or mutant Htt differ during homeostasis and stress? and (3) if differences exist, how does cytoplasmic mHtt expression affect secretory protein folding in the ER lumen?

Results

Differential effect of Htt^{ex1} and full-length Htt on induction of ER stress

We began by investigating whether UPR was present in cells expressing mHtt. We expressed a cytotoxic truncated form of mHtt. Mice expressing the first exon 1 (Htt^{ex1}) of mHtt develop rapid and severe disease symptoms, similar to HD pathology (Mangiarini et al., 1996). Htt^{ex1} includes the first 67 amino acids of full-length Htt with the internal stretch of a variable number of glutamines. However, the exon1 peptide does not occur naturally and its relevance to understanding full-length mHtt pathology is an ongoing debate in HD research (Truant et al., 2008). We transiently transfected differentiated Neuro-2a (N2a) cells with Htt^{ex1} constructs tagged with GFP and containing various lengths of polyQ (23, 73 and 145).These cells were harvested 48 hours post-transfection, processed for immunoblotting, and probed for the UPR hallmark, increased levels of BiP (Fig. 1A). The disease-associated Q73 and Q145 $mHtt^{ex1}$ constructs did not exhibit significant increases in BiP levels compared with non-pathological Q23 or untransfected cells treated with an ER stressor, tunicamycin (Tm). Similar results were observed with anti-BiP and anti-CHOP immunofluorescence analyses (supplementary material Fig. S1). Our findings contrasted with a report of upregulated BiP and other UPR markers (i.e. phosphorylated eIF2α and CHOP) (Reijonen et al., 2008) in PC6.3 cells transiently expressing Htt^{ex1}. Immunoblot results for transiently transfected cells depend on transfection efficiency. Therefore, we analyzed single cells for the expression of a fluorescent reporter under the control of the ER stress response element (ERSE) of the BiP promoter (ERSE tdTomato). Expression of the reporter, as measured by mean cell fluorescence intensity was significantly induced upon treatment of N2a cells with the positive control Tm (Fig. 1B,C; supplementary material Fig. S2). Coexpression of the reporter with either GFP alone or various Htt^{ex1}–GFP constructs revealed that both Q73 and Q145 induced increased expression of the ERSE tdTomato reporter compared with Q23 (Fig. 1B,C). However, induction was significantly lower than the level observed in cells expressing GFP alone that were treated with Tm. Thus, Htt^{ex1} expression does induce UPR in N2a cells.

The physiological relevance of overexpression of Htt^{ex1} is controversial. To examine a more physiological model of mHtt expression, we used mouse striatal cell lines expressing two knockin copies of full-length wild-type (seven glutamines; $STHdh^{Q7/7}$) or mutant (111 glutamines; $STHdh^{Q111/111}$) Htt under the endogenous promoter (Trettel et al., 2000). BiP levels in untreated $STHdh^{Q7/7}$ and $STHdh^{Q111/111}$ cell lysates were also analyzed by immunoblot (Fig. 2A). No difference was observed between the two cell lines. Immunofluorescence analysis of these cells with anti-BiP and anti-CHOP (Fig. 2B) also failed to provide evidence of robust UPR activity. Moreover, no difference was observed between $STHdh^{Q7/7}$ and $STHdh^{Q111/111}$ cells when transfected with the ERSE tdTomato reporter. Increased expression of the reporter was observed with the positive control of $STHdh^{Q7/7}$ cells treated with Tm (Fig. 2C). Thus, mHtt possibly only induces a modest UPR in tissue culture cell models, unlike the extreme stress of Tm treatment. Such a mild phenotype might require more sensitive detection methods or even more pathologic forms of mHtt to amplify the phenotype. Indeed, Duennwald and Lindquist only detected UPR activation in yeast cells expressing a more toxic synthetic form of Htt^{ex1} lacking an internal proline domain (Duennwald and Lindquist, 2008).

The underlying basis of UPR activation is increased levels of unfolded proteins. To detect changes in the unfolded protein burden in cells, we employed an assay recently developed in our lab to measure changes in the mobility of the chaperone BiP in live cells (Lai et al., 2010). Under stress conditions, BiP–GFP increasingly binds to unfolded or misfolded proteins, significantly increasing the molecular size relative to unbound BiP (Fig. 3A). Changes in molecular size can be detected as changes in molecular mobility using fluorescence microscopy techniques (Snapp et al., 2003a). Using a laser scanning confocal microscope, fluorescence recovery after photobleaching (FRAP) can be performed by irreversibly photobleaching a fluorescent protein in a region of interest (ROI) in a cell with a high-intensity

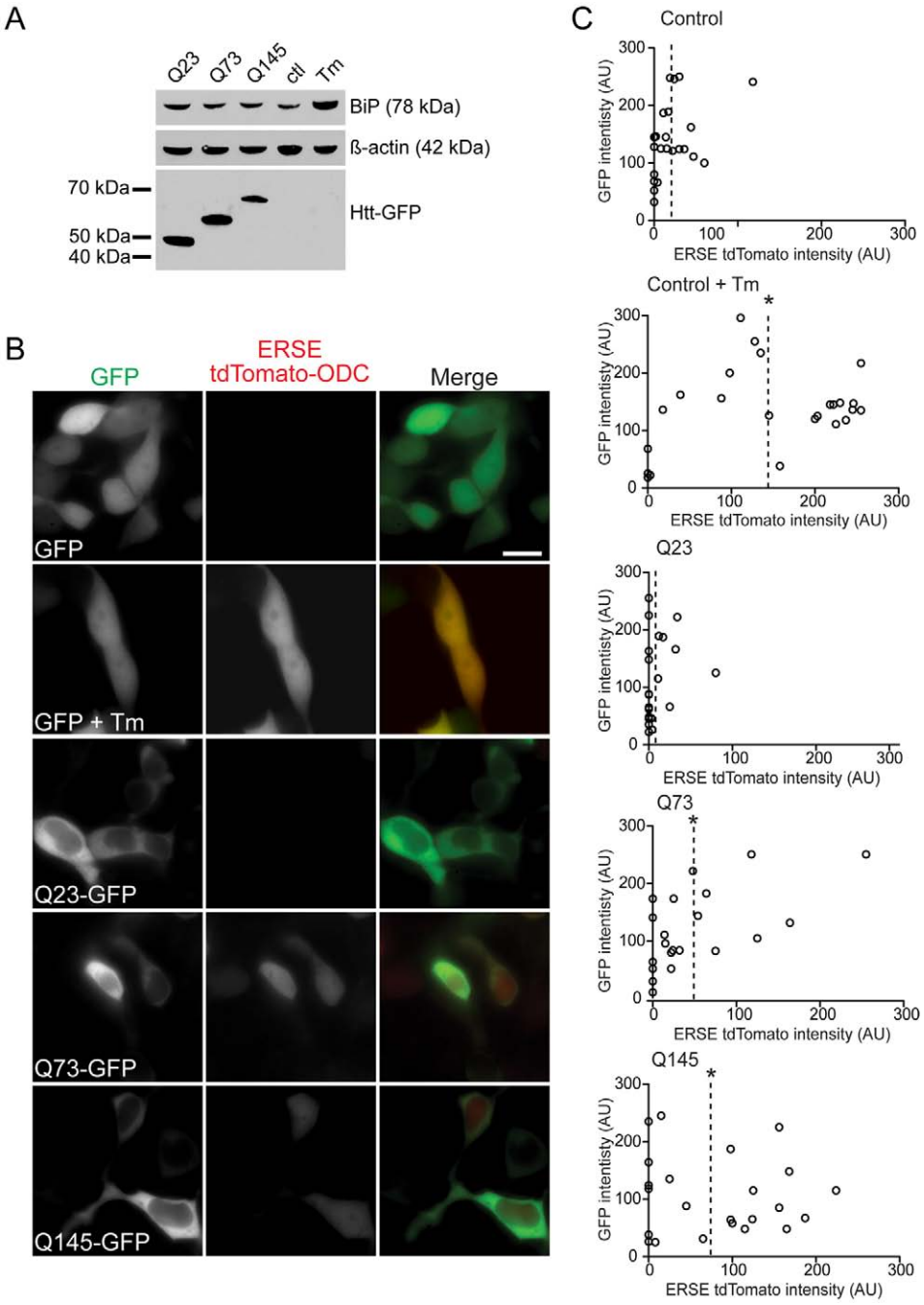

Fig. 1. Analysis of the ER stress marker BiP in Htt^{ex1}–GFP-transfected cells. (**A**) Immunoblot of BiP levels in N2a cells transiently transfected with Htt^{ex1}–GFP vectors containing 23, 73 or 145 polyQ repeats for 16 hours. Untransfected cells treated with 5 µg/ml Tm for 8 h or left untreated as a control. Samples were lysed and separated by SDS-PAGE and immunoblotted with anti-BiP or anti-GFP. Equal loading was confirmed by reprobing with anti-β-actin. (**B**) Representative fluorescence images of N2a cells transiently co-transfected with either empty GFP or Htt^{ex1}–GFP and ERSE tdTomato ODC vectors. A positive control was included of cells expressing GFP and ERSE TdTomato ODC treated with 5 µg/ml Tm for 16 hours. Scale bars: 20 µm. (**C**) N2a cells were transiently co-transfected with either empty GFP or Htt^{ex1}–GFP and ERSE tdTomato ODC vectors. A positive control (as for B) was included. Plots show fluorescence intensities of both GFP, or Htt^{ex1}–GFP, and ERSE TdTomato ODC for individual cells. *P<0.01; AU, arbitrary units.

laser beam and then monitoring diffusion of unbleached fluorescent molecules into the bleached ROI (Lippincott-Schwartz et al., 2001; Snapp et al., 2003a). The recovery rate can be used to calculate the effective diffusion coefficient (D) (Siggia et al., 2000). The major parameters affecting protein mobility are the viscosity of the environment and the hydrodynamic radius of the protein (Einstein, 1905). BiP is mobile within the ER lumen and a slower fluorescence recovery can be observed over time, relative to the much faster recovery of the smaller inert probe, ER–GFP, under the same conditions (Fig. 3B) (Lai et al., 2010). We used FRAP of BiP–GFP to investigate changes in the ER environment of mHtt-expressing cells. First, N2a cells were co-transfected with BiP–GFP and Htt^{ex1}–mCherry vectors and analyzed by FRAP. To minimize the number of cells with IBs, experiments were carried 16 hours post-transfection, although no difference was observed between cells containing or lacking IBs (supplementary material Fig. S3). Cells expressing Q73 or Q145 mHtt^{ex1} exhibited significant decreases in BiP–GFP mobility compared with Q23-expressing cells. This decrease was comparable with that in N2a cells treated with Tm (Fig. 3C). No clear correlation was observed between BiP–GFP mobility and Htt^{ex1} expression levels (supplementary material Fig. S4) suggesting that additional factors besides mHtt expression could be responsible for the variations of BiP–GFP mobility between cells (i.e. differences in proteasome or ERAD activity). Moreover, no significant changes were observed for the

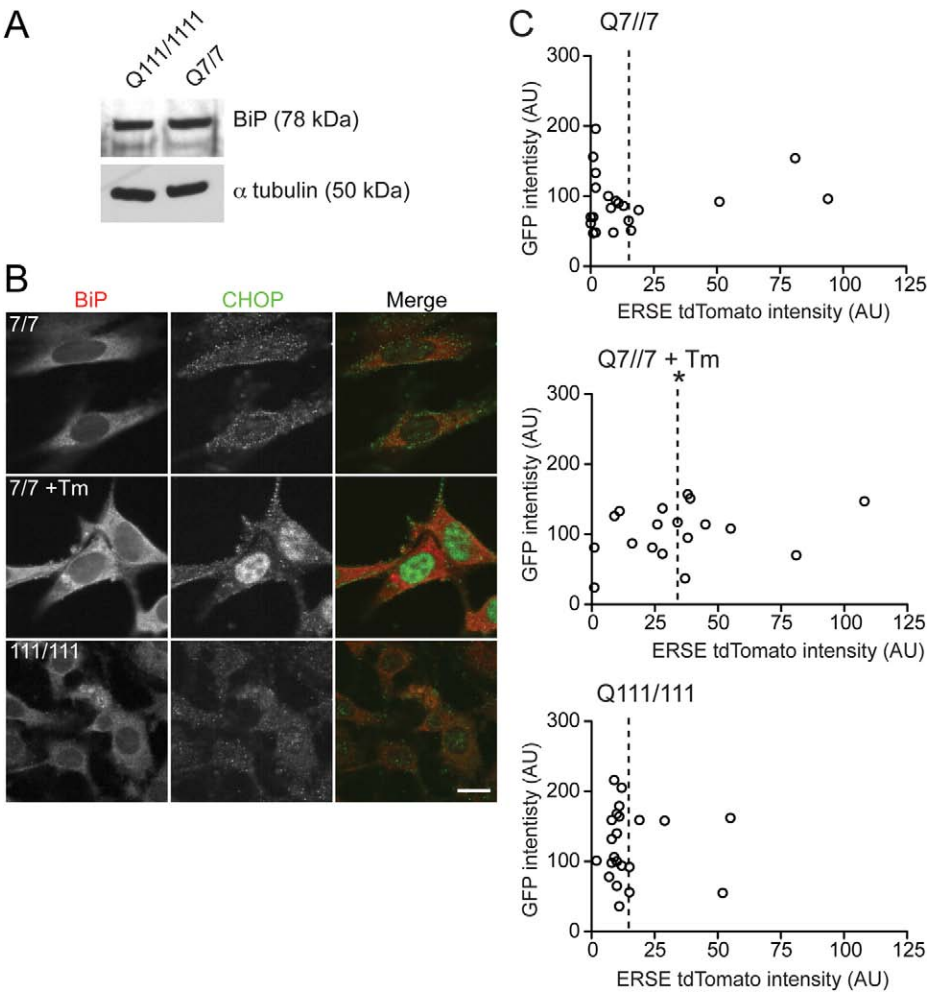

Fig. 2. Analysis of ER stress markers BiP and CHOP in STHdh$^{Q7/7}$ and STHdh$^{Q111/111}$ cells. (**A**) Immunoblot of BiP levels in STHdh$^{Q7/7}$ and STHdh$^{Q111/111}$ cells. Equal loading was confirmed by reprobing with anti-α-tubulin. (**B**) Representative fluorescence images of STHdh$^{Q7/7}$ and STHdh$^{Q111/111}$ cells untreated or treated with 5 μg/ml Tm for 16 hours and immunofluorescently labeled with anti-BiP and anti-CHOP. Scale bars: 20 μm. (**C**) STHdh$^{Q7/7}$ and STHdh$^{Q111/111}$ cells were transiently co-transfected with empty GFP and ERSE tdTomato ODC vectors. A positive control was included of STHdh$^{Q7/7}$ cells treated with 5 μg/ml Tm for 16 hours. Plots show fluorescence intensities of both GFP, or Htt^{ex1}–GFP, and ERSE TdTomato ODC for individual cells. *$P<0.01$; AU, arbitrary units.

ER–GFP inert probes, indicating the absence of gross changes to ER viscosity (Fig. 3D). Thus, consistent with the ERSE reporter, expression of mHtt^{ex1} significantly decreased BiP availability. Taken together these results indicate that cytoplasmic mHttex1 disrupts ER homeostasis.

Second, we examined whether stable expression of the full-length form of mHtt has similar effects on the luminal ER environment. STHdh$^{Q7/7}$ and STHdh$^{Q111/111}$ cells were transiently transfected with BiP–GFP or ER–GFP constructs. Unlike the results with mHtt^{ex1}, no significant changes in mobility of either protein were observed in the two cell types (Fig. 3E,F). One hypothesis for this discrepancy in results is STHdh cells express Htt at near endogenous levels, which are substantially lower than the levels of the transiently expressed exon 1 fragment. In addition, the Htt^{ex1} experiments acutely expose cells to a potentially stressful protein, whereas the STHdh cells constitutively express mutant protein and might be adapted to low level stress.

Increased sensitivity of mHtt expressing cells to acute stress

Although the STHdh cells might not exhibit overt ER stress, we hypothesized that the cells could be more susceptible to stress (Duennwald and Lindquist, 2008) or even partially adapted to stress as a form of hormesis (Mattson, 2008). To test for stress sensitivity, we compared the viability of STHdh$^{Q7/7}$ and STHdh$^{Q111/111}$ cells exposed to Tm ER stress and then stained the cells with anti-cleaved caspase-3 antibody to detect apoptosis (Fig. 4A,B). Alternatively, samples were processed for immunoblotting for cleaved caspase-3 (Fig. 4C). Both assays showed that in STHdh$^{Q111/111}$ cells apoptotic cell death was higher with prolonged treatment. A previous report described increased cell death from a pharmacologically unrelated ER stressor, thapsigargin, an inhibitor of the ER calcium sarco(endo)plasmic reticulum Ca^{2+}-ATPase (SERCA) pump (Duennwald and Lindquist, 2008). Thus, mHtt expression sensitizes striatal cells to ER stressors. These data suggest that ER stress exacerbates mHtt toxicity, increases cell susceptibility to normally tolerated stresses, and could play an important role in mHtt-induced neuronal cell death in vivo. Indeed, inhibition of apoptosis signal regulating kinase 1 (Ask1) activity, in the striatum reduces ER stress and can simultaneously alleviate motor dysfunction symptoms in HD mice (Cho et al., 2009).

To determine whether mHtt affects early stress events, we used the BiP–GFP mobility assay to monitor changes in BiP occupancy in STHdh$^{Q7/7}$ and STHdh$^{Q111/111}$ cells during acute Tm stress. Surprisingly, after only 30 minutes of Tm treatment, BiP mobility significantly decreased in STHdh$^{Q111/111}$ cells, whereas no change was observed at this time in STHdh$^{Q7/7}$ cells (Fig. 5A). The rate of decrease of BiP mobility was substantially

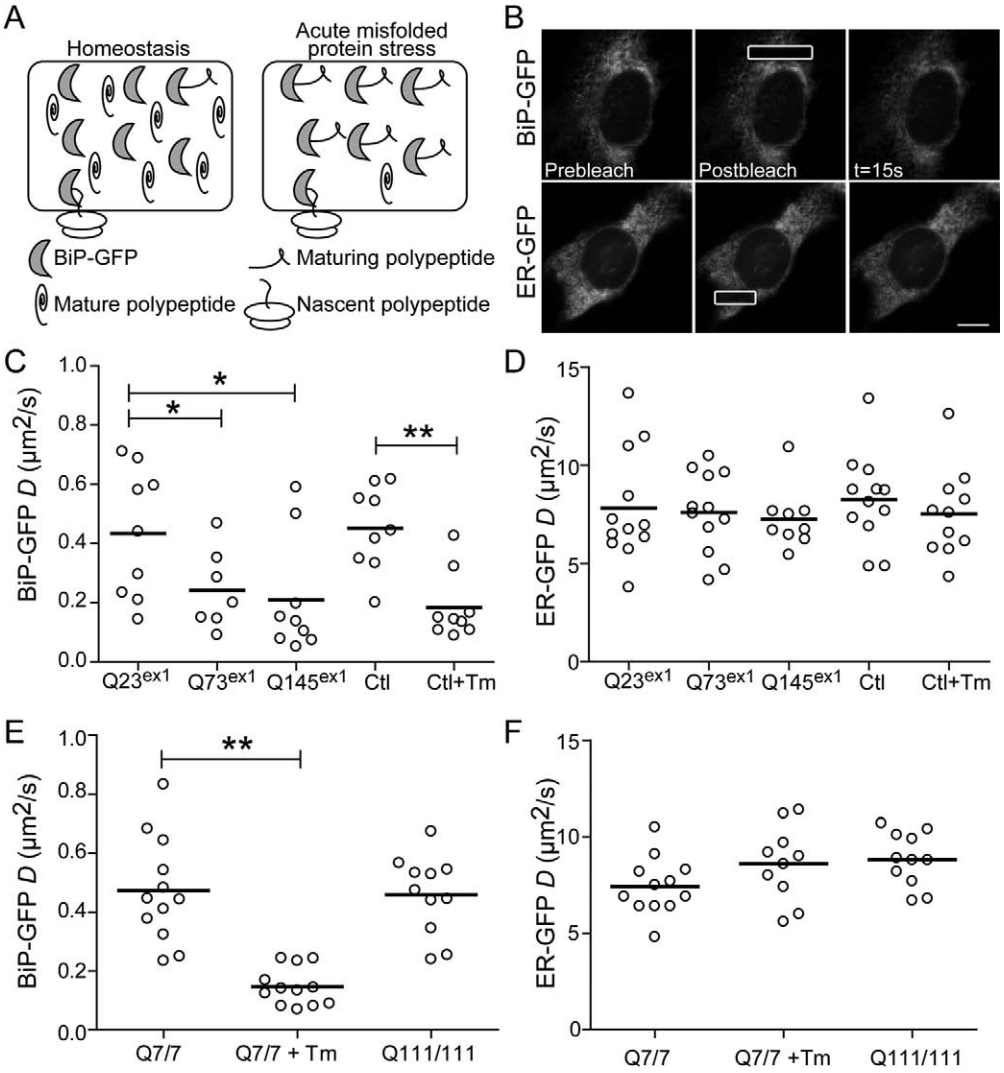

Fig. 3. Differential effect of expression of Htt^{ex1} and full-length Htt on the ER misfolded protein burden. (**A**) Illustration of how BiP availability distinguishes between states of homeostasis and stress. Upon acute ER stress, BiP–GFP binds to misfolded protein resulting in larger molecular complexes. An increase in complex size should result in decreased diffusional mobility. (**B**) Representative FRAP series of N2a cells transfected with either BiP–GFP or ER–GFP. Scale bars: 20 μm. (**C**,**D**) *D* values of individual N2a cells transiently co-transfected with Htt^{ex1}-mCherry constructs containing 23, 73 or 145 polyQ repeats and BiP–GFP (C) or ER–GFP (D) for 16 hours, and analyzed by FRAP. Control (Ctl) cells were transfected with BiP–GFP or ER–GFP alone and treated cells received 5 μg/ml Tm for 4 hours. (**E**,**F**) *D* values of individual STHdh$^{Q7/7}$ and STHdh$^{Q111/111}$ cells transfected with BiP–GFP or ER–GFP for 16 hours and treated with 5 μg/ml Tm for 4 hours or left untreated, and analyzed by FRAP. Thick horizontal lines in C–F indicate mean *D* values. *P<0.05 **P<0.001.

faster in STHdh$^{Q111/111}$ cells (Fig. 5B,C). No changes in *D* were detected for cells treated with DMSO alone (supplementary material Fig. S5).

We investigated whether this increased ER stressor sensitivity could be due to the presence of mHtt, the amount of mHtt and/or decreased levels of functional wild-type Htt. In addition to the two homozygous knockin strains, we obtained a heterozygote, STHdh$^{Q7/111}$, which exhibits milder mHtt pathology than the homozygous mutants (Trettel et al., 2000). This decreased activity might reflect a potentially protective role for wild-type Htt or decreased levels of cytotoxic mHtt in the heterozygous mutant cells (Trettel et al., 2000). In contrast to homozygotes, no acute changes in BiP–GFP mobility were observed in heterozygous cells after 30 minutes of Tm treatment (supplementary material Fig. S6). In a complementary experiment, overexpressing GFP-tagged full-length Htt in U2OS cells, which also express endogenous wild-type Htt, increased cell sensitivity to Tm (supplementary material Fig. S7). Together, these data suggest sensitivity to ER stressors depends on expression of mHtt, even in presence of the wild-type protein.

The FRAP results reflect more rapid accumulation of unfolded protein–BiP complexes in mutant cells compared with the wild-type counterpart. This effect was not a consequence of altered Tm potency to generate nonglycosylated proteins. The unglycosylated form of endogenous FGFR3 accumulated at the same rate in both cells lines upon Tm treatment (supplementary material Fig. S8). Importantly, the increased rate of BiP occupancy was not limited to Tm. Treatment of both cells lines with 2.5 mM dithiothreitol (DTT) also produced a faster decrease in BiP–GFP *D* for STHdh$^{Q111/111}$ cells compared with wild-type cells (Fig. 5D). No changes in mobility of the inert probe ER–RFP was observed in either cell line following treatment with either stressor, indicating that no significant changes in the ER viscosity occurred during the treatments (Fig. 5E). Because we had already observed no significant difference in levels of endogenous BiP in mutant and wild-type cells (Fig. 2A), our data suggest that in cells expressing mutant protein, BiP encounters higher levels of unfolded proteins in the ER lumen. This could reflect a decrease in flux of unfolded proteins out of the ER, possibly because of less efficient ERAD.

We predicted a faster rate of accumulation of unfolded proteins in mHtt-expressing cells would result in faster UPR activation. Indeed, during Tm treatment, the UPR was activated at least 2 hours earlier in STHdh$^{Q111/111}$ cells, as measured by the early UPR event, phosphorylation of eIF2α (Fig. 5F). This result indicates that rapid accumulation of misfolded protein in the ER of STHdh$^{Q111/111}$ cells correlates with activation of the UPR signaling cascade.

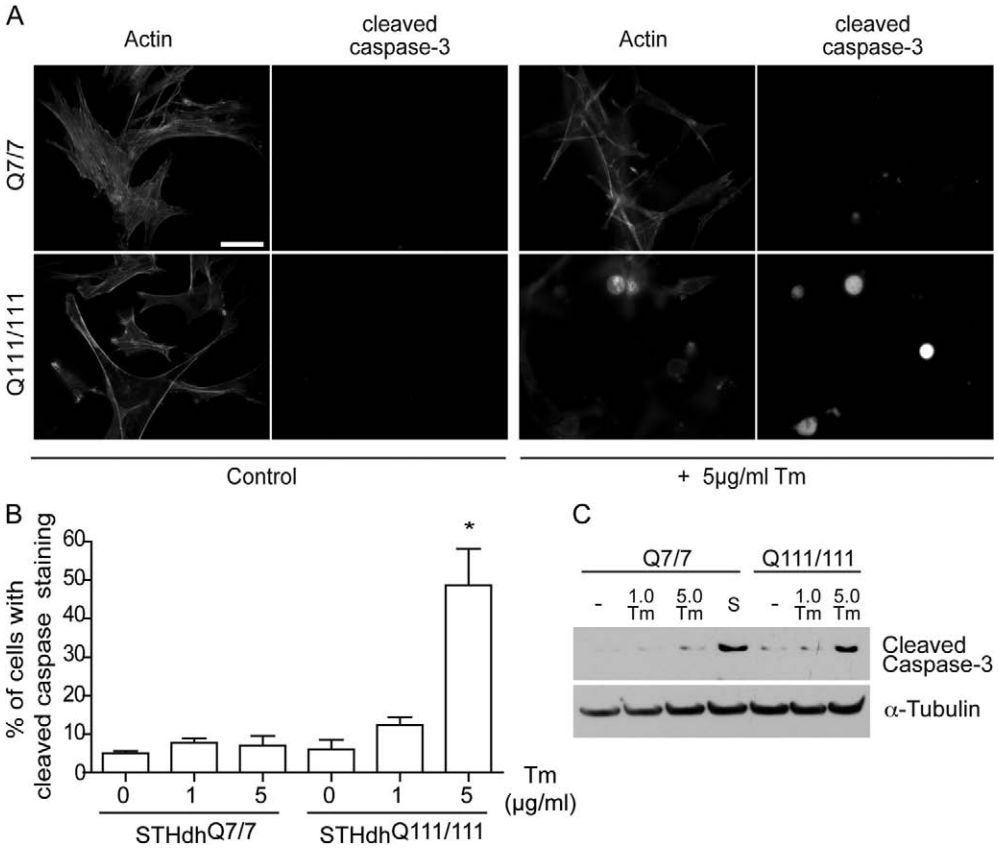

Fig. 4. mHtt expression is associated with increased ER stressor-induced cell death in striatal cells expressing full-length Htt. (**A**) STHdh$^{Q7/7}$ and STHdh$^{Q111/111}$ cells untreated (control) or treated with 5 μg/ml Tm for 16 hours. Cells were fixed and labeled with cleaved caspase-3 antibody and phalloidin. Scale bars: 20 μm. (**B**) The percentage of cells with cleaved caspase-3 staining. *$P<0.01$. (**C**) STHdh$^{Q7/7}$ and STHdh$^{Q111/111}$ cells treated with 1 (1.0 Tm) and 5 μg/ml Tm (5.0 Tm) for 16 hours. STHdh$^{Q7/7}$ cells were also treated with 5 μM staurosporine for 5 hours as positive control (S). Cells were processed for immunoblotting for cleaved caspase-3. Immunoblots were then reprobed with anti-α-tubulin as a loading control.

Recovery and adaptation of neuronal cell to ER stress

Cells can recover from acute misfolded protein stress (Rutkowski et al., 2006) and BiP substrates can disappear quickly after washout of a stressor, such as DTT (Lai et al., 2010; Lodish and Kong, 1993; Tatu et al., 1993). We investigated whether cells expressing mHtt can recover from acute misfolded protein accumulation, despite increased sensitivity to ER stressors. We performed the BiP–GFP FRAP assay on STHdh cells before, after a 30-minute treatment with 5 mM DTT and following a 1-hour washout of the drug. Both STHdh$^{Q7/7}$ and STHdh$^{Q111/111}$ cells exhibited significantly lower BiP–GFP mobility following the 30-minute DTT treatment (Fig. 6), similar to a previous report, although different cell types were used (Lai et al., 2010). Both cell lines exhibited similar recoveries after the 1-hour washout of DTT. The 1 hour time frame for complete recovery of BiP–GFP mobility indicates that most of the misfolded proteins are able to refold or are degraded (de Silva et al., 1993; Lai et al., 2010). Misfolded secretory proteins, such as the Null Hong Kong α1-antitrypsin mutant, exhibit ERAD-mediated turnover halftimes of at least 2 hours (Christianson et al., 2008; Kaytor et al., 2004; Svedine et al., 2004). Thus, even cells expressing mHtt can resolve unfolded protein burdens. In the context of the data in Fig. 5, these results suggest the QC machinery in mutant-protein-expressing cells can cope with BiP substrates at steady state, but become rapidly overwhelmed with even modest increases in BiP substrate levels.

These findings raised the question of whether we could improve the resistance of mHtt-expressing cells to ER stress. One possibility would be to adapt cells to ER stress by conditioning them with low doses of stress, which has been demonstrated to protect against more severe ER stress challenges (Rutkowski et al., 2006; Rutkowski and Kaufman, 2007). Adaptation increases overall secretory capacity and flux of the ER by upregulating chaperones, trafficking effectors (i.e. COPII machinery), and ERAD components (Lee et al., 2003). Using a similar approach, we treated both STHdh$^{Q7/7}$ and STHdh$^{Q111/111}$ cells with 5 mM DTT for 30 minutes, then washed out the drug for 16 hours, thus allowing the cells to recover and adapt. Cells were fixed and stained with anti-BiP to visualize any increase in stress-induced UPR-upregulated BiP levels. Consistent with previous studies, both STHdh$^{Q7/7}$ and STHdh$^{Q111/111}$ cells show increased BiP levels following DTT treatment (Fig. 7A). Thus, both wild-type and mHtt-expressing cells can adaptively upregulate BiP levels following ER stress. Adapted cells were then challenged with Tm, and BiP–GFP mobility was measured by FRAP. Consistent with the predicted adapted phenotype, BiP–GFP *D* values for STHdh$^{Q7/7}$ cells previously treated with DTT, did not significantly decrease when challenged with Tm, compared with untreated cells (Fig. 7B). By contrast, despite increased BiP levels in STHdh$^{Q111/111}$ cells pretreated with DTT, the cells still exhibited substantially slower BiP–GFP mobility following Tm challenge (Fig. 7B). Adapted STHdh$^{Q111/111}$ cells were still as sensitive to Tm and associated cell death as unadapted STHdh$^{Q111/111}$ cells (Fig. 7C). Thus, the adaptative response in these cells is not protective.

One potential explanation for this discrepancy is that not all aspects of the ER capacity for flux are increased by adaptation in mutant cells. Clearly, ER chaperone levels increased and it is

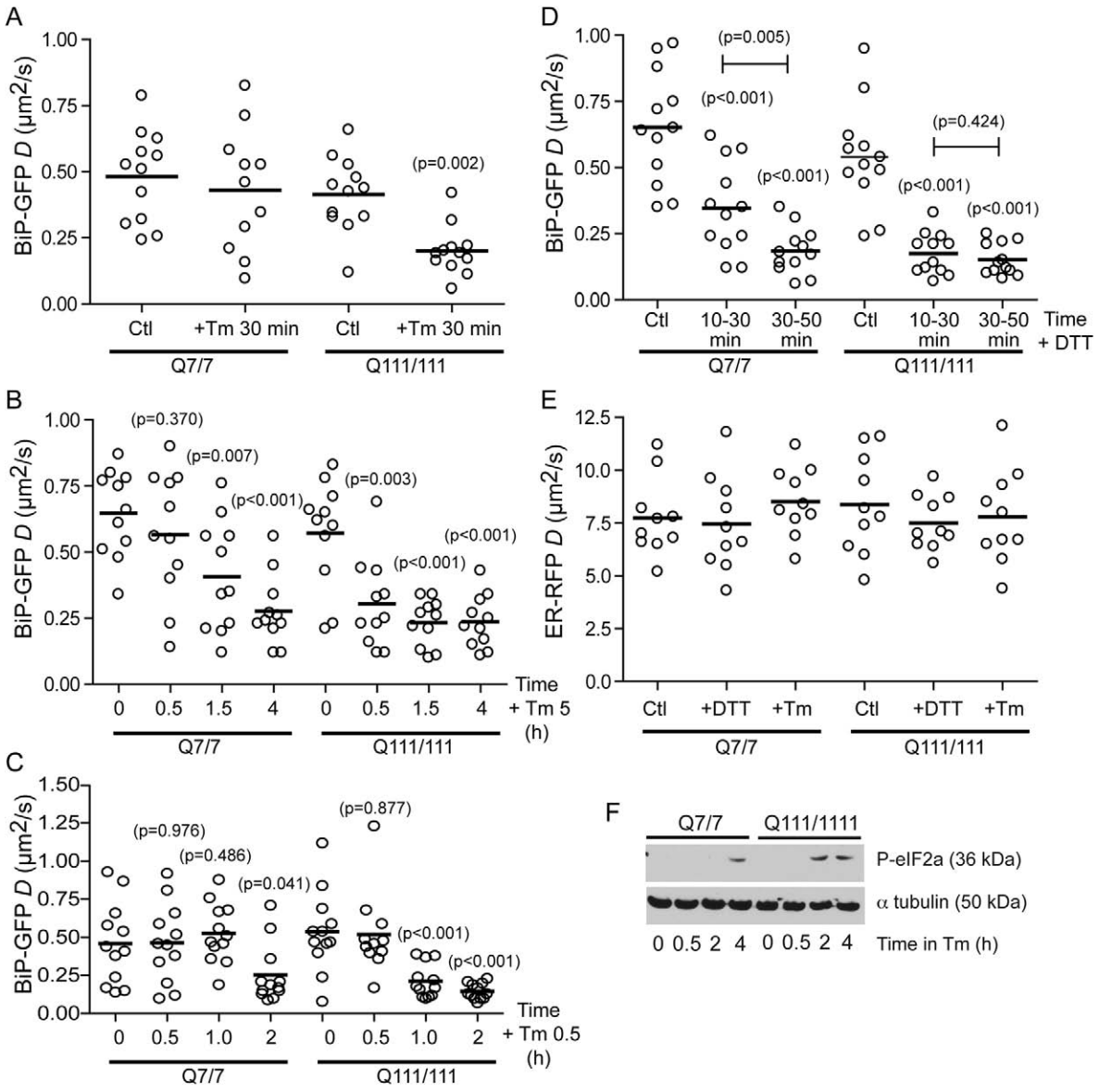

Fig. 5. BiP availability reveals increased sensitivity to ER stress in STHdh$^{Q111/111}$ cells. (**A**) *D* values of single STHdh$^{Q7/7}$ and STHdh$^{Q111/111}$ cells transfected with BiP–GFP for 16 hours, and either left untreated (Ctl) or treated with 5 μg/ml Tm for 30 minutes and analyzed by FRAP. (**B**) *D* values of single STHdh$^{Q7/7}$ and STHdh$^{Q111/111}$ cells transfected with BiP–GFP for 16 hours and treated with 5 μg/ml Tm for 30 minutes, 1.5 hours and 4 hours. (**C**) *D* values of single STHdh$^{Q7/7}$ and STHdh$^{Q111/111}$ cells transfected with BiP–GFP for 16 hours and treated with 0.5 μg/ml Tm for 30 minutes, 1 hour and 2 hours. (**D**) *D* values of single STHdh$^{Q7/7}$ and STHdh$^{Q111/111}$ cells transfected with BiP–GFP for 16 hours and treated with 2.5 mM DTT. *D* values are binned into 20 minutes intervals. (**E**) *D* values of single STHdh$^{Q7/7}$ and STHdh$^{Q111/111}$ cells transfected with inert ER–RFP for 16 hours and treated with either 2.5 mM DTT for 30 minutes or 5 μg/ml Tm for 4 hours and analyzed by FRAP. (**F**) Immunoblots of the UPR reporter phosphorylated eIF2α from STHdh$^{Q7/7}$ and STHdh$^{Q111/111}$ cells treated with 5 μg/ml Tm for the indicated times. Equal loading was confirmed by reprobing with anti-α-tubulin. Statistically significant differences between treated and untreated cells for the same cell line (unless otherwise specified) are shown in parentheses above the data sets.

likely the trafficking and ERAD machinery components are similarly increased, as they are all subject to regulation by the same transcription factors. A recent report from Duennwald and Lindquist described how expression of a modified mHtt^{ex1} construct in both yeast and mammalian cells impaired ERAD (Duennwald and Lindquist, 2008). A decrease in ERAD capacity would be predicted to slow flux of unfolded proteins out of the ER during stress, leading to more rapid accumulation during treatment with stressors. Whether full-length mHtt impairs ERAD in striatal cells is unknown. We investigated whether STHdh$^{Q111/111}$ cells exhibit impaired ERAD compared with wild-type cells. Because striatal cells are difficult to transfect, biochemical analysis of ERAD substrate degradation is challenging at best. Therefore, we utilized live-cell imaging, which does not require the high transfection efficiencies of standard biochemical approaches. Cells were transiently transfected with superfolder (SF)GFP-tagged CD3δ and ER–RFP. Alternatively, cells were transiently transfected with ER–RFP and an inert ER membrane marker, P450–GFP (Snapp et al., 2003b). The ratio of P450–GFP/ER–RFP mean intensities was

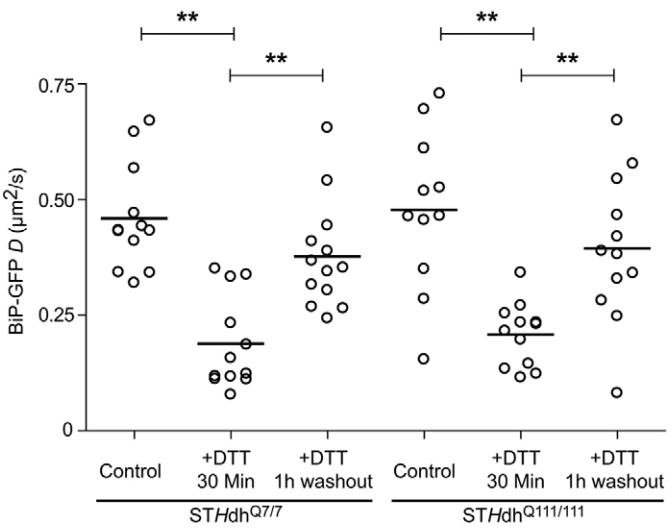

Fig. 6. Reversibility of misfolded protein stress on BiP–GFP mobility in striatal cell. *D* values of single STHdh$^{Q7/7}$ and STHdh$^{Q111/111}$ cells transfected with BiP–GFP for 16 hours and treated with 5 mM DTT for 30 minutes followed by a 1-hour washout of the drug in one well and analyzed by FRAP. *P<0.01.

the same for the two cells lines (Fig. 8A,B). By contrast the ratio of CD3δ to ER–RFP levels significantly increased in STHdh$^{Q111/111}$ cells relative to STHdh$^{Q7/7}$ cells, consistent with decreased clearance of the ERAD substrate in mHtt-expressing cells. Thus, impaired turnover of misfolded protein upon acute ER stress is likely to be important to the mechanism underlying the increased sensitivity of STHdh$^{Q111/111}$ cells to ER stressors.

Discussion

HD patients typically do not present with clinical symptoms until middle age and patients with the same number of pathologic polyglutamines exhibit a wide range of ages of onset (±19 years for most lengths of polyQ) (Gusella and MacDonald, 2006). Therefore, HD severity and pathology must depend on naturally occurring modifiers. In this study, we found mHtt expression increased cell vulnerability to misfolded secretory protein stressors. We demonstrated that striatal cells expressing mHtt are more sensitive to pharmacological ER stressors, leading to faster accumulation of BiP substrates in the ER of these cells and more rapid activation of UPR signaling. Importantly, these cells exhibited a decreased ability to adapt following sub-lethal dose of a stressor. As a consequence, mutant or misfolded secretory proteins that would otherwise be tolerated in wild-type cells could be potential modifiers of mHtt toxicity and pathology. Such proteins could accumulate and activate apoptotic ER stress pathways or could titrate QC factors and impair the folding of other secretory proteins, similar to the effects in the cytoplasm caused by overexpressed polyglutamine expansions (Gidalevitz et al., 2006; Rutkowski and Kaufman, 2007). Enhanced sensitivity to ER stress is consistent with a model of a progressive HD pathology. The presence of mHtt does not acutely or even necessarily directly kill cells. Instead, mHtt expression can increase cell susceptibility to various stresses. Over years of continuous exposure to stressors, vulnerable cells will prematurely succumb to normally tolerated stresses. Extrapolating from our study, patients with a mutant misfolded copy of a neuronal

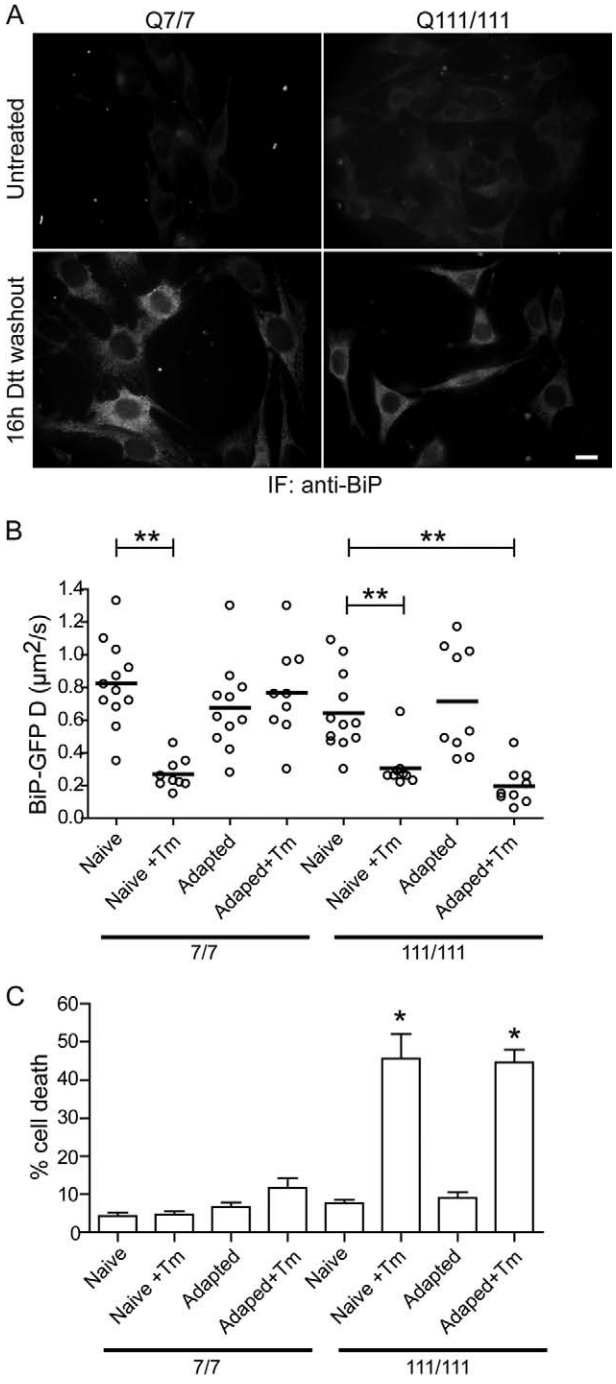

Fig. 7. Adaptation to ER stress in striatal cells expressing full-length Htt. (**A**) Representative fluorescence images of STHdh$^{Q7/7}$ and STHdh$^{Q111/111}$ cells either left untreated or treated with 5 mM DTT for 30 minutes and followed by 16 hours washout of the drug. Cells were fixed and immunofluorescently stained with anti-BiP. Scale bar: 20 μm. (**B**) *D* values of single STHdh$^{Q7/7}$ and STHdh$^{Q111/111}$ cells transfected with BiP–GFP for 16 hours, and either left untreated (Naive) or treated with 5 mM DTT for 30 minutes (Adapted) and followed by a 16-hour washout of the drug. Naive or Adapted cells were subsequently challenged with 5 μg/ml Tm for 4 hours (+Tm), and analyzed by FRAP. (**C**) STHdh$^{Q7/7}$ and STHdh$^{Q111/111}$ cells either left untreated (Naive) or treated with 5 mM DTT for 30 minutes (Adapted) and followed by a 16-hour washout of the drug. Naive or Adapted cells were subsequently challenged with 5 μg/ml Tm for 16 hours, fixed and labeled with anti-cleaved caspase-3 and phalloidin. The percentage of cells with cleaved caspase staining was then determined. n>82 cells per data set. *P<0.01, **P<0.0005.

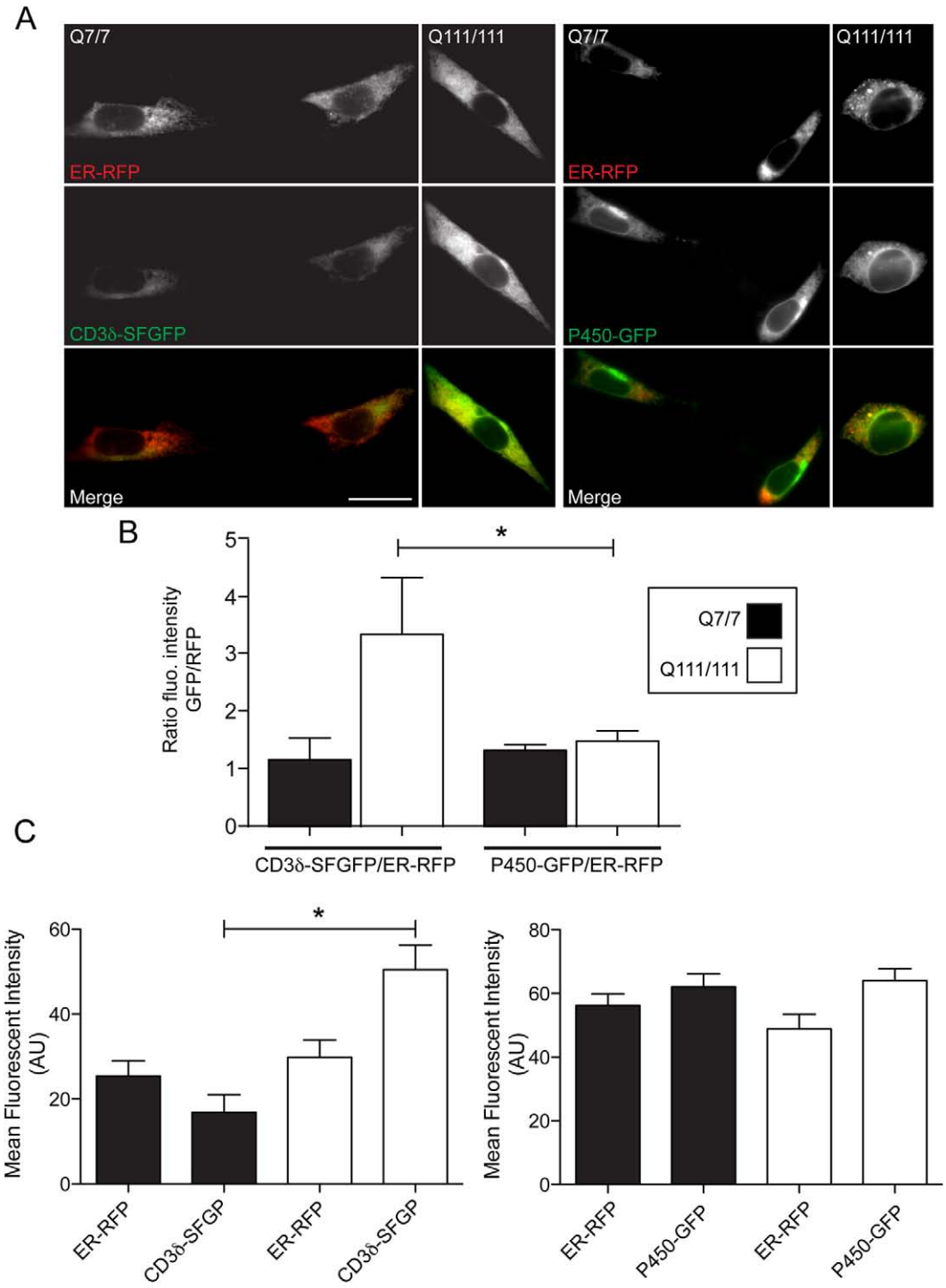

Fig. 8. Accumulation of ERAD substrate in striatal cells expressing mHTT. (**A**) Representative fluorescence images of STHdh$^{Q7/7}$ and STHdh$^{Q111/111}$ cells co-transfected with either CD3δ–SFGFP or P450–GFP (green) and ER–RFP (red). Merge images are shown in the bottom panel. Scale bar: 20 μm. (**B**) The ratios of CD3δ–SFGFP/ER–RFP and P450–GFP/ER–RFP fluorescence intensities in STHdh$^{Q7/7}$ and STHdh$^{Q111/111}$ cells. (**C**) Mean fluorescent intensities of CD3δ–SFGFP, P450–GFP and ER–RFP in STHdh$^{Q7/7}$ and STHdh$^{Q111/111}$ cells. *$P<0.05$; $n>25$ cells for each data set.

secretory protein could experience consequential levels of UPR activation, whereas a person lacking an expanded polyglutamine mHtt would successfully cope with the same mutant misfolded protein without experiencing significant ER stress.

The mechanism of increased sensitivity to ER stressors appears to be complex. We observed no evidence of ER stress at steady state in striatal neuronal cells expressing endogenous levels of full-length mHtt. Thus, the presence of mHtt does not cause constitutive UPR activation. An important caveat is that patients typically present with only one mutant copy of mHtt, so our model cells probably represent an extreme of the spectrum of mHtt expression levels for patients. The more physiological heterozygous striatal

neurons were not detectably sensitive to acute ER stress in the way the Q111/111 homozygotes were (supplementary material Fig. S6). However, there are several issues with knockin mouse models of HD, not least of which is that only homozygotes exhibit HD-like phenotypes and then only in old age and with considerably longer polyQ regions than those associated with HD onset in humans (Ehrnhoefer et al., 2009). Therefore, it will be important to extend our studies to human striatal cells, if possible.

A clue for the likely underlying mechanism of increased sensitivity to ER stressors came with the finding that mHtt expression decreased rates of turnover of an ERAD substrate. This finding fits well with previous reports of decreased activity of the ubiquitin-proteasome system (UPS) in mHtt-expressing cells (Bennett et al., 2007; Godin et al., 2010; Tydlacka et al., 2008). The proteasome is a key component of ERAD and the flux of misfolded proteins out of the ER. Inhibition of the proteasome blocks the degradation of ERAD substrates, such as CD3δ (Tiwari and Weissman, 2001), and the dislocation of several ERAD substrates (Mancini et al., 2000; Musil et al., 2000; VanSlyke et al., 2000). Furthermore, ERAD effector proteins p97/Np14/Ufd1 and gp78 have been reported to interact with and be sequestered by mHtt, establishing a link between polyQ toxicity and ER stress (Duennwald and Lindquist, 2008; Yang et al., 2010). Similarly, interaction of other cytoplasmic polyQ proteins, in particular ataxin 3 (AT3), with ERAD machinery has been reported. These interactions lead to accumulation of ERAD substrates in AT3-expressing cells (Boeddrich et al., 2006; Zhong and Pittman, 2006). In light of these findings, even if the UPR is activated and the levels of ERAD components can be upregulated, mHtt inhibition of ERAD components and proteasomal activity would still limit ERAD activity. Interestingly, we found that simply inhibiting proteasomal degradation using MG132 was not sufficient to induce changes in BiP–GFP mobility in the absence of ER stress (supplementary material Fig. S9).

The absence of stress at steady state in the STHdh$^{111/111}$ cells suggests the cells have adapted to decreased ERAD flux. Translation or transcription might be attenuated to decrease the flux of incoming nascent proteins to accommodate the lower rate of ERAD in these cells. In yeast, translational dysfunction has been observed coincident with mHtt^{ex1} expression (Tauber et al., 2011). For diseases such as HD, the inability of cells to cope with ER stress could represent an important modulator of the mutant protein toxicity. In future studies, it will be interesting to monitor changes in misfolded protein accumulation in the ER of mHtt-expressing cells not only under prolonged stress, but also during aging. Investigating differences in how these cells regulate early events after exposure to ER stress will help characterize the role of the UPR in HD and its potential as a therapeutic target.

Materials and Methods

Chemicals

Dithiothreitol (DTT; Fisher Scientific, Pittsburgh, PA) was diluted to the indicated concentrations from a 1 M stock solution in water. Tunicamycin (TM; Calbiochem, LaJolla, CA) was diluted to the indicated concentrations from a 5 mg/ml stock solution in DMSO.

Cell lines

U2OS and Neuro-2a (N2a) cells were obtained from ATCC. STHdh$^{Q7/7}$, STHdh^{Q7111} and STHdh$^{Q111/111}$ cells (Trettel et al., 2000) were obtained from Coriell Cell Repository (Camden, NJ). All cells were grown in eight-well Lab-tek chambers (Nunc; Rochester, NY) in RPMI medium (Mediatech; Manassas, VA) containing 10% fetal bovine serum (Hyclone from Thermo Scientific; Rockford, IL), glutamine and penicillin–streptomycin (Invitrogen; Carlsbad, CA). STHdh cells were grown in a 5% CO_2 incubator at 33℃ as previously described (Trettel et al., 2000), whereas U2OS and N2a cells were grown in a 5% CO_2 incubator at 37℃. N2a cells were routinely differentiated by incubating the cells with 5 µM dbcAMP (N69, 29-*O*-dibutyrilaenosine-39:59-cyclic monophosphate sodium salt; Sigma-Aldrich; St. Louis, MO) for 2 days (Jana et al., 2000).

Tissue culture conditions can impact ER stress pathway activation. Duennwald and Lindquist reported that STHdh$^{Q111/111}$ cells show increased expression of ER stress markers such as BiP and CHOP (Duennwald and Lindquist, 2008). They cultured the cells at 39℃ to inhibit proliferation. FRAP analysis of both STHdh$^{Q7/7}$ and STHdh$^{Q111/111}$ cells transfected with BiP–GFP at 39℃ produced no significant difference in BiP–GFP mobility (supplementary material Fig. S10). It is possible that cell proliferation and differentiation states influences ER stress induction in these cells. For example Trettel et al. induce neuronal differentiation using a protocol involving serum starvation and forskolin treatment (Trettel et al., 2000). The latter can induce upregulation of BiP (Cunha et al., 2009).

Constructs and transfection

Construction of Htt^{ex1}Q23, Htt^{ex1}Q73 and Htt^{ex1}Q145 fused to mGFP or mCherry, ER-DEVD-tdTomato (Lajoie and Snapp, 2010) and ER–GFP and ER–RFP (Snapp et al., 2006) plasmids was described previously. Full-length Htt–GFP constructs were made with template plasmids, obtained from Coriell and cloned into pcDNA 3.1 (Invitrogen). The sequence encoding the N-terminal end of full-length Htt with either 23 or 145 repeats up to the first internal *Kpn*I site were amplified by PCR using the following primers: forward 5′-GATCTCCGGAGCGACCCTGGAAAAG-3′, and reverse 5′-GATCGGTACCGTCTAACA-3′. The fragments were then cloned into the *Bsp*EI–*Kpn*I sites of monomeric pEGFP-C1 (Clontech) to generate GFP–(*Kpn*I). *Sna*BI–*Kpn*1 fragments were cloned from GFP–(*Kpn*I) Htt into the *Sna*BI–*Kpn*1 sites of the parental pcDNA Htt plasmids. Plasmids were transfected into cells using Lipofectamine 2000 (Invitrogen) according to the manufacturer's instructions. CD3δ–SFGP was made by insertion of mouse CD3δ into an N1-SFGFP plasmid (Pedelacq et al., 2006). The ornithine decarboxylase sequence was amplified by PCR using the following primers: forward 5′-GATCTGTACAAATTCCCGCCGGAGGTG-3′ and reverse 5′-GATCGCGGCCGCTTAGTGACGGTCCATCCC-3′ and the fragment was cloned into the *Bsr*GI–*Not*I sites of tdTomato-N1. ERSE TdTomato ODC was made with BiP-169 luciferase template plasmid obtained from Tom Rutkowski (Molecular & Cellular Biology Program, University of Iowa, Iowa City, IA) and fused to the PEST sequence of mouse ornithine decarboxylase (ODC) to enhance fluorescent protein turnover. The BiP ERSE promoter region (–169 to –29) was amplified by PCR using the following primers: forward 5′-GATCATTAATGTACTTGGAGCGGCC-3′ and reverse 5′-GATC-GAATTCAAGCTTACTTAGATC-3′. The fragment was then cloned into tdTomato ODC-N1 using the *Ase*I–*Eco*RI sites.

FRAP

Live cells were imaged in Phenol Red–free RPMI supplemented with 10 mM Hepes and 10% FBS, imaged at 37℃ or 33℃ (according to the cell line), on a Duoscan confocal microscope system (Carl Zeiss Microimaging) with a 633 NA 1.4 oil objective, a 489 nm 100 mW diode laser with a 500–550 nm bandpass filter for GFP, and a 40 mW 561 nm diode laser with a 565 longpass filter for mRFP and tdTomato. FRAP experiments were performed by photobleaching an ROI at full laser power of the 489 nm line and monitoring fluorescence recovery over time. No photobleaching of the adjacent cells during the processes was observed. *D* measurements were calculated as described previously (Siggia et al., 2000; Snapp et al., 2003a). Statistical analyses using Student's *t*-test were performed with Prism 5.0c (GraphPad Software Inc., La Jolla CA).

Quantitative fluorescence microscopy

Cells were fixed with freshly diluted 3.7% formaldehyde in PBS for 15 minutes at room temperature, permeabilized with 0.1% Triton X-100 in 1× PBS, and blocked with 10% fetal bovine serum in 13 PBS. Cells were labeled with anti-cleaved caspase-3 (Cell Signaling Technology Inc., Danvers, MA), anti-BiP (Santa Cruz Biotechnology Inc., Santa Cruz, CA), followed by Alexa-Fluor-488-or Alexa-Fluor-555-conjugated anti-rabbit IgG secondary antibodies (Invitrogen). Some cells were stained with Alexa-Fluor-555-conjugated phalloidin (Invitrogen). Cells were imaged using an Axiovert 200 widefield fluorescence microscope (Carl Zeiss Microimaging Inc.) with a 633 oil immersion 1.4 NA objective, and 470/40 excitation, 525/50 emission bandpass filter for GFP and Alexa Fluor 488, and 565/30 excitation, 620/60 emission bandpass filter for Alexa Fluor 555, mRFP and tdTomato. Image analysis was performed with ImageJ (National Institutes of Health; Bethesda, MD). Statistical analyses using Student's *t*-test were performed with Prism 5.0c.

Immunoblots

N2a and STHdh cells were grown in 12-well tissue-culture-treated plates (Corning Inc., Corning, NY), rinsed twice with PBS, and lysed in 30 µl sample buffer (1% SDS, 0.1 M Tris, pH 8.0), run on 12% Tris–tricine gels, and transferred to nitrocellulose

membrane. Antibodies used included anti-GFP (a generous gift from Ramanujan S. Hegde, National Institutes of Health), anti-BiP (Santa Cruz Biotechnology Inc.), anti-phosphorylated eIF2α (Epitomics Inc., Burlingame, CA), anti-α-tubulin and anti-β-actin (Sigma Aldrich, St Louis, MO), anti-FGFR3 (Santa Cruz) and HRP-labeled anti-rabbit or anti-mouse (Jackson Immunoresearch Laboratories) or anti-goat (Santa Cruz Biotechnology Inc.) secondary antibodies. All images for figures were prepared using Photoshop CS4 and Illustrator CS4 (Adobe Systems, San Jose, CA).

Acknowledgements

We thank Ramanujan S. Hegde for the anti-GFP antibody. This study was supported by an Early Discovery Initiative grant from CHDI, NIA R21 1R21AG032544-01, and NIGMS R01GM086530–01 to E.L.S.

Supplementary material available online at
http://jcs.biologists.org/lookup/suppl/doi:10.1242/jcs.087510/-/DC1

References

Bennett, E. J., Shaler, T. A., Woodman, B., Ryu, K. Y., Zaitseva, T. S., Becker, C. H., Bates, G. P., Schulman, H. and Kopito, R. R. (2007). Global changes to the ubiquitin system in Huntington's disease. *Nature* **448**, 704-708.

Bernales, S., McDonald, K. L. and Walter, P. (2006). Autophagy counterbalances endoplasmic reticulum expansion during the unfolded protein response. *PLoS Biol.* **4**, e423.

Boeddrich, A., Gaumer, S., Haacke, A., Tzvetkov, N., Albrecht, M., Evert, B. O., Muller, E. C., Lurz, R., Breuer, P., Schugardt, N. et al. (2006). An arginine/lysine-rich motif is crucial for VCP/p97-mediated modulation of ataxin-3 fibrillogenesis. *EMBO J.* **25**, 1547-1558.

Carnemolla, A., Fossale, E., Agostoni, E., Michelazzi, S., Calligaris, R., De Maso, L., Del Sal, G., MacDonald, M. E. and Persichetti, F. (2009). Rrs1 is involved in endoplasmic reticulum stress response in Huntington disease. *J. Biol. Chem.* **284**, 18167-18173.

Caviston, J. P. and Holzbaur, E. L. (2009). Huntingtin as an essential integrator of intracellular vesicular trafficking. *Trends Cell Biol.* **19**, 147-155.

Chen, S., Berthelier, V., Yang, W. and Wetzel, R. (2001). Polyglutamine aggregation behavior in vitro supports a recruitment mechanism of cytotoxicity. *J. Mol. Biol.* **311**, 173-182.

Cho, K. J., Lee, B. I., Cheon, S. Y., Kim, H. W., Kim, H. J. and Kim, G. W. (2009). Inhibition of apoptosis signal-regulating kinase 1 reduces endoplasmic reticulum stress and nuclear huntingtin fragments in a mouse model of Huntington disease. *Neuroscience* **163**, 1128-1134.

Christianson, J. C., Shaler, T. A., Tyler, R. E. and Kopito, R. R. (2008). OS-9 and GRP94 deliver mutant alpha1-antitrypsin to the Hrd1-SEL1L ubiquitin ligase complex for ERAD. *Nat. Cell Biol.* **10**, 272-282.

Cunha, D. A., Ladriere, L., Ortis, F., Igoillo-Esteve, M., Gurzov, E. N., Lupi, R., Marchetti, P., Eizirik, D. L. and Cnop, M. (2009). Glucagon-like peptide-1 agonists protect pancreatic beta-cells from lipotoxic endoplasmic reticulum stress through upregulation of BiP and JunB. *Diabetes* **58**, 2851-2862.

de Silva, A., Braakman, I. and Helenius, A. (1993). Posttranslational folding of vesicular stomatitis virus G protein in the ER: involvement of noncovalent and covalent complexes. *J. Cell Biol.* **120**, 647-655.

Duennwald, M. L. and Lindquist, S. (2008). Impaired ERAD and ER stress are early and specific events in polyglutamine toxicity. *Genes Dev.* **22**, 3308-3319.

Ehrnhoefer, D. E., Butland, S. L., Pouladi, M. A. and Hayden, M. R. (2009). Mouse models of Huntington disease: variations on a theme. *Dis. Model. Mech.* **2**, 123-129.

Einstein, A. (1905). Über die von der molekularkinetischen Theorie der Wärme geforderte Bewegung von in ruhenden Flüssigkeiten suspendierten Teilchen. *Ann. Phys.* **17**, 549-560.

Finkbeiner, S. and Mitra, S. (2008). The ubiquitin-proteasome pathway in Huntington's disease. *ScientificWorldJournal* **8**, 421-433.

Gidalevitz, T., Ben-Zvi, A., Ho, K. H., Brignull, H. R. and Morimoto, R. I. (2006). Progressive disruption of cellular protein folding in models of polyglutamine diseases. *Science* **311**, 1471-1474.

Godin, J. D., Poizat, G., Hickey, M. A., Maschat, F. and Humbert, S. (2010). Mutant huntingtin-impaired degradation of beta-catenin causes neurotoxicity in Huntington's disease. *EMBO J.* **29**, 2433-2445.

Gregersen, N. and Bross, P. (2010). Protein misfolding and cellular stress: an overview. *Methods Mol. Biol.* **648**, 3-23.

Gusella, J. F. and MacDonald, M. E. (2006). Huntington's disease: seeing the pathogenic process through a genetic lens. *Trends Biochem. Sci.* **31**, 533-540.

Harding, H. P., Zhang, Y. and Ron, D. (1999). Protein translation and folding are coupled by an endoplasmic-reticulum-resident kinase. *Nature* **397**, 271-274.

Higashio, H. and Kohno, K. (2002). A genetic link between the unfolded protein response and vesicle formation from the endoplasmic reticulum. *Biochem. Biophys. Res. Commun.* **296**, 568-574.

Hosoi, T. and Ozawa, K. (2010). Endoplasmic reticulum stress in disease: mechanisms and therapeutic opportunities. *Clin. Sci.* **118**, 19-29.

Jana, N. R., Tanaka, M., Wang, G. and Nukina, N. (2000). Polyglutamine length-dependent interaction of Hsp40 and Hsp70 family chaperones with truncated N-terminal huntingtin: their role in suppression of aggregation and cellular toxicity. *Hum. Mol. Genet.* **9**, 2009-2018.

Kaytor, M. D., Wilkinson, K. D. and Warren, S. T. (2004). Modulating huntingtin half-life alters polyglutamine-dependent aggregate formation and cell toxicity. *J. Neurochem.* **89**, 962-973.

Kouroku, Y., Fujita, E., Jimbo, A., Kikuchi, T., Yamagata, T., Momoi, M. Y., Kominami, E., Kuida, K., Sakamaki, K., Yonehara, S. et al. (2002). Polyglutamine aggregates stimulate ER stress signals and caspase-12 activation. *Hum. Mol. Genet.* **11**, 1505-1515.

Kozutsumi, Y., Segal, M., Normington, K., Gething, M. J. and Sambrook, J. (1988). The presence of malfolded proteins in the endoplasmic reticulum signals the induction of glucose-regulated proteins. *Nature* **332**, 462-464.

Lai, C. W., Aronson, D. E. and Snapp, E. L. (2010). BiP availability distinguishes states of homeostasis and stress in the endoplasmic reticulum of living cells. *Mol. Biol. Cell* **21**, 1909-1921.

Lajoie, P. and Snapp, E. L. (2010). Formation and toxicity of soluble polyglutamine oligomers in living cells. *PLoS ONE* **5**, e15245.

Lee, A. H., Iwakoshi, N. N. and Glimcher, L. H. (2003). XBP-1 regulates a subset of endoplasmic reticulum resident chaperone genes in the unfolded protein response. *Mol. Cell. Biol.* **23**, 7448-7459.

Lippincott-Schwartz, J., Snapp, E. and Kenworthy, A. (2001). Studying protein dynamics in living cells. *Nat. Rev. Mol. Cell Biol.* **2**, 444-456.

Lodish, H. F. and Kong, N. (1993). The secretory pathway is normal in dithiothreitol-treated cells, but disulfide-bonded proteins are reduced and reversibly retained in the endoplasmic reticulum. *J. Biol. Chem.* **268**, 20598-20605.

Mancini, R., Fagioli, C., Fra, A. M., Maggioni, C. and Sitia, R. (2000). Degradation of unassembled soluble Ig subunits by cytosolic proteasomes: evidence that retrotranslocation and degradation are coupled events. *FASEB J.* **14**, 769-778.

Mangiarini, L., Sathasivam, K., Seller, M., Cozens, B., Harper, A., Hetherington, C., Lawton, M., Trottier, Y., Lehrach, H., Davies, S. W. et al. (1996). Exon 1 of the HD gene with an expanded CAG repeat is sufficient to cause a progressive neurological phenotype in transgenic mice. *Cell* **87**, 493-506.

Marciniak, S. J. and Ron, D. (2006). Endoplasmic reticulum stress signaling in disease. *Physiol. Rev.* **86**, 1133-1149.

Martinez, I. M. and Chrispeels, M. J. (2003). Genomic analysis of the unfolded protein response in *Arabidopsis* shows its connection to important cellular processes. *Plant Cell* **15**, 561-576.

Mattson, M. P. (2008). Hormesis defined. *Ageing Res. Rev.* **7**, 1-7.

Meusser, B., Hirsch, C., Jarosch, E. and Sommer, T. (2005). ERAD: the long road to destruction. *Nat. Cell Biol.* **7**, 766-772.

Musil, L. S., Le, A. C., VanSlyke, J. K. and Roberts, L. M. (2000). Regulation of connexin degradation as a mechanism to increase gap junction assembly and function. *J. Biol. Chem.* **275**, 25207-25215.

Nishitoh, H., Matsuzawa, A., Tobiume, K., Saegusa, K., Takeda, K., Inoue, K., Hori, S., Kakizuka, A. and Ichijo, H. (2002). ASK1 is essential for endoplasmic reticulum stress-induced neuronal cell death triggered by expanded polyglutamine repeats. *Genes Dev.* **16**, 1345-1355.

Noh, J. Y., Lee, H., Song, S., Kim, N. S., Im, W., Kim, M., Seo, H., Chung, C. W., Chang, J. W., Ferrante, R. J. et al. (2009). SCAMP5 links endoplasmic reticulum stress to the accumulation of expanded polyglutamine protein aggregates via endocytosis inhibition. *J. Biol. Chem.* **284**, 11318-11325.

Oliveira, J. M. (2010). Nature and cause of mitochondrial dysfunction in Huntington's disease: focusing on huntingtin and the striatum. *J. Neurochem.* **114**, 1-12.

Ozcan, U., Yilmaz, E., Ozcan, L., Furuhashi, M., Vaillancourt, E., Smith, R. O., Gorgun, C. Z. and Hotamisligil, G. S. (2006). Chemical chaperones reduce ER stress and restore glucose homeostasis in a mouse model of type 2 diabetes. *Science* **313**, 1137-1140.

Pedelacq, J. D., Cabantous, S., Tran, T., Terwilliger, T. C. and Waldo, G. S. (2006). Engineering and characterization of a superfolder green fluorescent protein. *Nat. Biotechnol.* **24**, 79-88.

Reijonen, S., Putkonen, N., Norremolle, A., Lindholm, D. and Korhonen, L. (2008). Inhibition of endoplasmic reticulum stress counteracts neuronal cell death and protein aggregation caused by N-terminal mutant huntingtin proteins. *Exp. Cell Res.* **314**, 950-960.

Riley, B. E. and Orr, H. T. (2006). Polyglutamine neurodegenerative diseases and regulation of transcription: assembling the puzzle. *Genes Dev.* **20**, 2183-2192.

Ron, D. and Walter, P. (2007). Signal integration in the endoplasmic reticulum unfolded protein response. *Nat. Rev. Mol. Cell Biol.* **8**, 519-529.

Rutkowski, D. T. and Kaufman, R. J. (2007). That which does not kill me makes me stronger: adapting to chronic ER stress. *Trends Biochem. Sci.* **32**, 469-476.

Rutkowski, D. T., Arnold, S. M., Miller, C. N., Wu, J., Li, J., Gunnison, K. M., Mori, K., Sadighi Akha, A. A., Raden, D. and Kaufman, R. J. (2006). Adaptation to ER stress is mediated by differential stabilities of pro-survival and pro-apoptotic mRNAs and proteins. *PLoS Biol.* **4**, e374.

Scheper, W. and Hoozemans, J. J. (2009). Endoplasmic reticulum protein quality control in neurodegenerative disease: the good, the bad and the therapy. *Curr. Med. Chem.* **16**, 615-626.

Scherzinger, E., Sittler, A., Schweiger, K., Heiser, V., Lurz, R., Hasenbank, R., Bates, G. P., Lehrach, H. and Wanker, E. E. (1999). Self-assembly of polyglutamine-containing huntingtin fragments into amyloid-like fibrils: implications for Huntington's disease pathology. *Proc. Natl. Acad. Sci. USA* **96**, 4604-4609.

Schuck, S., Prinz, W. A., Thorn, K. S., Voss, C. and Walter, P. (2009). Membrane expansion alleviates endoplasmic reticulum stress independently of the unfolded protein response. *J. Cell Biol.* **187**, 525-536.

Siggia, E. D., Lippincott-Schwartz, J. and Bekiranov, S. (2000). Diffusion in inhomogeneous media: theory and simulations applied to whole cell photobleach recovery. *Biophys. J.* **79**, 1761-1770.

Snapp, E. L., Altan, N. and Lippincott-Schwartz, J. (2003a). Measuring protein mobility by photobleaching GFP chimeras in living cells. *Curr. Protoc. Cell Biol.* **Chapter 21**, Unit 21 1.

Snapp, E. L., Hegde, R. S., Francolini, M., Lombardo, F., Colombo, S., Pedrazzini, E., Borgese, N. and Lippincott-Schwartz, J. (2003b). Formation of stacked ER cisternae by low affinity protein interactions. *J. Cell Biol.* **163**, 257-269.

Snapp, E. L., Sharma, A., Lippincott-Schwartz, J. and Hegde, R. S. (2006). Monitoring chaperone engagement of substrates in the endoplasmic reticulum of live cells. *Proc. Natl. Acad. Sci. USA* **103**, 6536-6541.

Sturrock, A. and Leavitt, B. R. (2010). The clinical and genetic features of Huntington disease. *J. Geriatr. Psychiatry Neurol.* **23**, 243-259.

Svedine, S., Wang, T., Halaban, R. and Hebert, D. N. (2004). Carbohydrates act as sorting determinants in ER-associated degradation of tyrosinase. *J. Cell Sci.* **117**, 2937-2949.

Tabas, I. and Ron, D. (2011). Integrating the mechanisms of apoptosis induced by endoplasmic reticulum stress. *Nat. Cell Biol.* **13**, 184-190.

Tatu, U., Braakman, I. and Helenius, A. (1993). Membrane glycoprotein folding, oligomerization and intracellular transport: effects of dithiothreitol in living cells. *EMBO J.* **12**, 2151-2157.

Tauber, E., Miller-Fleming, L., Mason, R. P., Kwan, W., Clapp, J., Butler, N. J., Outeiro, T. F., Muchowski, P. J. and Giorgini, F. (2011). Functional gene expression profiling in yeast implicates translational dysfunction in mutant huntingtin toxicity. *J. Biol. Chem.* **286**, 410-419.

Thomas, M., Yu, Z., Dadgar, N., Varambally, S., Yu, J., Chinnaiyan, A. M. and Lieberman, A. P. (2005). The unfolded protein response modulates toxicity of the expanded glutamine androgen receptor. *J. Biol. Chem.* **280**, 21264-21271.

Tiwari, S. and Weissman, A. M. (2001). Endoplasmic reticulum (ER)-associated degradation of T cell receptor subunits. Involvement of ER-associated ubiquitin-conjugating enzymes (E2s). *J. Biol. Chem.* **276**, 16193-16200.

Trettel, F., Rigamonti, D., Hilditch-Maguire, P., Wheeler, V. C., Sharp, A. H., Persichetti, F., Cattaneo, E. and MacDonald, M. E. (2000). Dominant phenotypes produced by the HD mutation in STHdh(Q111) striatal cells. *Hum. Mol. Genet.* **9**, 2799-2809.

Truant, R., Atwal, R. S., Desmond, C., Munsie, L. and Tran, T. (2008). Huntington's disease: revisiting the aggregation hypothesis in polyglutamine neurodegenerative diseases. *FEBS J.* **275**, 4252-4262.

Tydlacka, S., Wang, C. E., Wang, X., Li, S. and Li, X. J. (2008). Differential activities of the ubiquitin-proteasome system in neurons versus glia may account for the preferential accumulation of misfolded proteins in neurons. *J. Neurosci.* **28**, 13285-13295.

VanSlyke, J. K., Deschenes, S. M. and Musil, L. S. (2000). Intracellular transport, assembly, and degradation of wild-type and disease-linked mutant gap junction proteins. *Mol. Biol. Cell* **11**, 1933-1946.

Yang, H., Liu, C., Zhong, Y., Luo, S., Monteiro, M. J. and Fang, S. (2010). Huntingtin interacts with the cue domain of gp78 and inhibits gp78 binding to ubiquitin and p97/VCP. *PLoS ONE* **5**, e8905.

Zhong, X. and Pittman, R. N. (2006). Ataxin-3 binds VCP/p97 and regulates retrotranslocation of ERAD substrates. *Hum. Mol. Genet.* **15**, 2409-2420.

Journal of Cell Science